

theory and the JS-BD theory, refute the argument of Bates²² explaining the "success" of the conventional first Born approximation. Bates has derived a matrix element similar to ours but argues that for moderate or large inter-proton distances the interaction $(R_{12}^{-1} + a_0^{-1}) \exp(-2R_{12}/a_0)$ is negligible compared with the interaction $R_{12}^{-1} - r_{1e}^{-1}$. But close encounters, as we have shown, are important in the capture process and the correction term cannot properly be dropped. Its inclusion changes the character of the interaction. In our opinion the "success" of either the JS-BD or our first-order theory in the intermediate energy range 35–200 keV still is not completely understood, because of the following (usually conveniently overlooked) difficulties: (i) In the classical limit the capture cross section should behave like v^{-11} at high velocities,⁶ whereas the BK, JS-BD, and our cross sections all behave like v^{-12} .

²² D. R. Bates, Proc. Roy. Soc. (London) **A247**, 294 (1958).

(ii) The impact parameter treatment of each of these theories shows that with increasing proton energy the cross section results from capture at smaller and smaller impact parameters, whereas physical expectation suggests capture should be possible for any proton passing through the electron cloud; in other words, although the total probability of capture decreases, there seems no reason why at high energies capture is possible only for those protons with vanishingly small impact parameters.

7. ACKNOWLEDGMENTS

We should like to thank Dr. T. M. Donahue and Dr. R. M. Drisko for many interesting discussions of the charge exchange problem, Dr. T. F. Tuan for transmitting his results of a calculation of capture from molecular hydrogen before publication, and Mr. B. D. Williams for his aid in the calculations.

Charge Transfer in Molecular Hydrogen*

T. F. TUAN,† *University of Pittsburgh, Pittsburgh, Pennsylvania*

AND

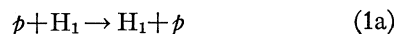
E. GERJUOY,‡ *General Atomic, San Diego, California*§

(Received August 17, 1959)

The effects of the molecule on electron capture by protons in hydrogen gas have been investigated in first Born approximation with different types of electronic wave functions. It always has been supposed that if the incident proton velocity is large compared to electronic velocities molecular effects may be neglected, and that one may then assume one H₂ molecule is equivalent to two hydrogen atoms for purposes of charge transfer. Instead it appears that charge transfer in H₂ at high energies bears no simple relationship to charge transfer in atomic hydrogen. In particular, among other effects: (i) in the high-energy limit $\frac{1}{2}\sigma_M = 1.2 - 1.4\sigma_A$; (ii) at lower energies there is important interference between the capture amplitudes from the two atoms in the molecule. It also is found that transitions to ungerade states of H₂⁺, although unimportant in the energy range of present experiments, become appreciable at high energies.

1. INTRODUCTION

THE theoretical problem of the charge transfer reaction



has received considerable attention from a large number

of investigators.¹⁻⁹ In the energy range from about 10² eV to 10⁴ eV, the cross section σ_A for the above reaction has been measured by crossed beam techniques.¹⁰ There are, however, no data available at energies well above 10 keV where the Born approxima-

* Submitted to the Graduate Faculty, University of Pittsburgh, in partial fulfillment of the requirements for the Ph.D. degree. The work was supported in part by the Office of Naval Research, and in part under a joint General Atomic-Texas Atomic Energy Research Foundation program on controlled thermonuclear reactions.

† Present address, Physics Department, Northwestern University, Evanston, Illinois.

‡ On leave from the University of Pittsburgh, Pittsburgh, Pennsylvania.

§ John Jay Hopkins Laboratory for Pure and Applied Science, General Atomic Division of General Dynamics Corporation, San Diego, California.

¹ L. H. Thomas, Proc. Roy. Soc. (London) **114**, 561 (1927).

² H. C. Brinkman and H. A. Kramers, Proc. Acad. Sci. Amsterdam **33**, 973 (1930).

³ D. R. Bates and A. Dalgarno, Proc. Phys. Soc. (London) **A65**, 919 (1952); and **A66**, 972 (1953).

⁴ J. D. Jackson and H. Schiff, Phys. Rev. **89**, 359 (1953).

⁵ H. Schiff, Can. J. Phys. **32**, 393 (1954).

⁶ R. Drisko, thesis, Carnegie Institute of Technology, 1955 (unpublished).

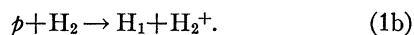
⁷ T. Pradhan, Phys. Rev. **105**, 1250 (1957).

⁸ J. D. Jackson, Proc. Phys. Soc. (London) **A70**, 26 (1957).

⁹ R. H. Bassel and E. Gerjuoy, preceding paper, Phys. Rev. **117**, 749 (1960).

¹⁰ Fite, Brackmann, and Snow, Phys. Rev. **112**, 1161 (1958).

tion is supposed to be valid. At these higher energies, it has been customary to compare the theoretical predictions for the reaction (1a) with the experimental cross section¹¹⁻¹⁵ σ_M for charge transfer from H_2 molecules,



The comparison has been based on the assumption that at high energies (for the purpose of charge transfer) one hydrogen molecule is equivalent to two hydrogen atoms, i.e., that $\sigma_A = \frac{1}{2}\sigma_M$. It is the purpose of this paper to show that the above assumption is valid, if it is valid at all, only as a result of accidental cancellation of a number of molecular effects which have no analog in the atomic reaction (1a).

Our formulation of the reaction (1b) will be given in Sec. 2. In Sec. 3 we physically interpret the several different types of matrix elements contributing to the cross section σ_M , and find interference occurs between the two capture amplitudes from the two atomic centers in the molecule. This interference is especially important at energies $< \sim 1$ Mev, and of course has no analog in the atomic reaction (1a). In Sec. 4 we evaluate the first Born approximation contribution to σ_M from the interaction between the incident proton and the electron it captures. This contribution, which we term σ_{MBK} because it is the molecular analog of the contribution to σ_A evaluated by Brinkman and Kramers² (BK), is relatively readily computed at all energies. As will be seen σ_{ABK} is indeed very close to $\frac{1}{2}\sigma_{MBK}$ at energies < 400 kev, but only because of accidental compensation of the following effects: (i) the aforementioned interference, which is constructive for transitions to the ground H_2^+ state; (ii) the fact that the capture amplitude is approximately proportional to the probability that the electron being captured has the velocity of the incident proton, which probability is higher in the more tightly bound H_2 molecule than in atomic H; (iii) the relatively small probability of capture transitions to the ungerade dissociating states of H_2^+ . In connection with (iii) we remark that the transition probability to ungerade states is rigorously zero at all energies if extreme molecular orbital wave functions are employed, and therefore hardly can be large with any reasonable choice of molecular wave function. Since charge transfer from two isolated hydrogen atoms could equally well leave the remaining electron in the gerade or ungerade states, this reduced capture transition probability to ungerade states would cause $\frac{1}{2}\sigma_{MBK}$ to be approximately $\frac{1}{2}\sigma_{ABK}$, were it not for effects (i) and (ii) which increase σ_{MBK} relative to σ_{ABK} .

The assertion, that the result $\frac{1}{2}\sigma_{MBK} = \sigma_{ABK}$ at energies < 400 kev is accidental, is made because: (a) in the

very high-energy limit, as the incident proton velocity $v \rightarrow \infty$, the interference effect (i) washes out, but the effect (ii) becomes so important that $\frac{1}{2}\sigma_{MBK} \rightarrow 1.2\sigma_{ABK}$ to $1.4\sigma_{ABK}$, depending on the molecular wave function employed; (b) at energies above 400 kev, where the interference for transition to the gerade state first becomes destructive, $\frac{1}{2}\sigma_{MBK}$ becomes significantly less than σ_{ABK} . It is noteworthy that the dip in our computed σ_{MBK} at energies above 400 kev closely reproduces the shape of the experimental curve in this energy range (see Sec. 4). In fact, when $\frac{1}{2}\sigma_{MBK}$ is multiplied by the ratio $\sigma_{AJS}/\sigma_{ABK}$, where σ_{AJS} is the cross section for (1a) taking into account the proton-proton interaction,^{3,4} the computed quantity $\frac{1}{2}\sigma_{MJS} = (\sigma_{AJS}/\sigma_{ABK})\frac{1}{2}\sigma_{MBK}$ falls right on the experimental curve. This procedure for estimating the molecular analog of the Jackson and Schiff (JS) matrix elements for (1a) is adopted because exact evaluation of the contribution to σ_M from proton-proton interactions is arduous (though possible in closed form); moreover in our opinion the proton-proton contribution to σ_A is not yet well understood.⁹ For this latter reason, and also because this estimate of $\frac{1}{2}\sigma_M$ wholly neglects the contribution to σ_M from the interaction between the proton and the second (not captured) electron, the close agreement between the magnitudes of $\frac{1}{2}\sigma_{MJS}$ (computed as explained) and the experimental $\frac{1}{2}\sigma_M$ probably should not be taken too seriously; again of course, the second electron-proton contribution has no analog in the atomic reaction (1a). On the other hand the aforementioned agreement between the shapes of $\frac{1}{2}\sigma_{MBK}$ or $\frac{1}{2}\sigma_{MJS}$ and the experimental curve probably represents a real verification of the interference effect, which is expected for the molecular proton-proton as well as proton-electron contributions. The proton-proton contributions to σ_M in the limit $v \rightarrow \infty$ are computed directly from the matrix elements in Sec. 5. The ratio of $\frac{1}{2}\sigma_{MJS}$ to σ_{AJS} in this limit is almost exactly equal to $\frac{1}{2}\sigma_{MBK}/\sigma_{ABK}$, thus bearing out our assertion that the closer agreement at lower energies between σ_{AJS} and $\frac{1}{2}$ the experimental σ_M results from accidental cancellations of molecular effects; the near equality of $\frac{1}{2}\sigma_{MJS}/\sigma_{AJS}$ and $\frac{1}{2}\sigma_{MBK}/\sigma_{ABK}$ at $v \rightarrow \infty$ also justifies estimating $\frac{1}{2}\sigma_{MJS}$ at lower energies from $(\sigma_{AJS}/\sigma_{ABK})\frac{1}{2}\sigma_{MBK}$, assuming σ_{AJS} correctly represents the proton-proton contributions to (1a).

To check the validity of our conclusions, three types of molecular wave functions have been used throughout: the extreme atomic orbital,¹⁶ the extreme molecular orbital, and the Weinbaum.¹⁷ Although these wave functions give quite different binding energies and internuclear distances, they make relatively little difference in our computations, except in transitions to ungerade H_2^+ states. These transitions are examined in a final brief Sec. 6; the results suggest that measurement of the percentage dissociation following capture in the

¹¹ J. P. Keene, Phil Mag. **40**, 369 (1949).

¹² A. C. Whittier, Can. J. Phys. **32**, 275 (1954).

¹³ J. B. H. Stedeford and J. B. Hasted, Proc. Roy. Soc. (London) **A227**, 466 (1955).

¹⁴ C. F. Barnett and H. K. Reynolds, Phys. Rev. **109**, 355 (1958).

¹⁵ Curran, Donahue, and Kasner, Phys. Rev. **114**, 490 (1959).

¹⁶ S. C. Wang, Phys. Rev. **31**, 597 (1928).

¹⁷ S. Weinbaum, J. Chem. Phys. **1**, 593 (1933).

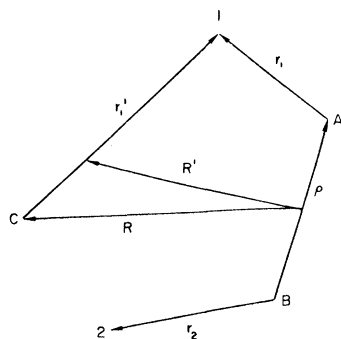


FIG. 1. Diagram showing the coordinate system. The letters represent the three protons, while the numbers represent the electrons.

reaction (1b) can provide a sensitive test of the interference effect we have predicted, and even can yield direct information on the ionic character of the ground state H_2 wave function.

2. FORMULATION

The coordinate system used is shown in Fig. 1. The electrons are 1 and 2, protons A and B are in the molecule and C is the incident proton. \mathbf{R} is the position of C relative to the center of mass of the H_2 molecule; \mathbf{R}' is the position of the center of mass of the outgoing hydrogen atom composed of C and 1, relative to the center of mass of the remaining H_2^+ ion containing particles A , B , and 2; ρ is the internuclear distance between the two nuclear protons A and B . The rest of the notations are relative coordinates and should be self-explanatory from the diagram, e.g., \mathbf{r}_1' is the position of 1 relative to C .

Since the incident proton in our problem has velocities greater than the velocity of the two electrons which themselves have much higher velocity than the two nuclear protons, we neglect the motion of the nuclear protons and take their separation to be the equilibrium distance of the hydrogen molecule. Moreover the two nuclear protons will be assumed infinitely massive.¹⁸ As is well known, whether or not the electrons are distinguishable, the total probability of capturing the electrons is the sum of the probabilities of capturing electron 1 and 2; this follows readily from the expression for the total flow of scattered particles at infinity, obtained in a time independent treatment of many-particle rearrangement collisions.¹⁹ In the present problem (1b) this makes the total probability of capturing electrons equal to twice the probability—computed as if the electrons were distinguishable—of capturing electron 1.

Thus in first Born approximation the center-of-mass system differential cross section, averaged over all orientations of ρ , the internuclear distance of the hydro-

¹⁸ Assuming the proton centers infinitely massive does not change the total cross section, N. F. Mott, Proc. Cambridge Phil. Soc. **27**, 553 (1931), although it makes the angular distribution in the center-of-mass system more sharply peaked in the forward direction.

¹⁹ E. Gerjuoy, Ann. Phys. **5**, 58 (1958).

gen molecule, is given by

$$\frac{d\sigma_M}{d\Omega} = 2 \frac{\mu_a \mu_b}{(2\pi\hbar^2)^2} \frac{K_b}{K_a} \frac{1}{4\pi} \int |\langle \psi_b | V_i | \psi_a \rangle|^2 d\Omega_\rho, \quad (2)$$

where V_i is the initial "prior" interaction; a and b always refer, respectively, to the initial and final unperturbed states given by

$$\begin{aligned} \psi_a &\doteq e^{i\mathbf{K}_a \cdot \mathbf{R}} \phi_m(\mathbf{r}_1, \mathbf{r}_2; \rho), \\ \psi_b &= e^{i\mathbf{K}_b \cdot \mathbf{R}'} \phi_i(\mathbf{r}_2; \rho) u(\mathbf{r}_1'); \end{aligned} \quad (3)$$

$K_a = \mu_a v / \hbar$; $K_b = \mu_b v_b / \hbar$; v is the incident proton velocity in the laboratory system; m is the electron mass; μ_a and μ_b equal, respectively, the initial and final reduced masses; v_b is the relative velocity after collision; ϕ_m denotes the molecular wave function; ϕ_i denotes the ion wave function; u is the ground-state atomic wave function; and

$$\mathbf{R} = \mathbf{r}_1 - \mathbf{r}_1' + \rho/2, \quad (4)$$

$$\mathbf{R}' = \mathbf{r}_1 - [M/(M+m)]\mathbf{r}_1' + \rho/2. \quad (5)$$

The wave function for the hydrogen molecule has the form

$$\begin{aligned} \phi_m(\mathbf{r}_1, \mathbf{r}_2; \rho) &= N_m \{ u_{mA}(1) u_{mB}(2) + u_{mA}(2) u_{mB}(1) \\ &\quad + c [u_{mA}(1) u_{mA}(2) + u_{mB}(1) u_{mB}(2)] \}, \quad (6) \\ N_m &= 1 / \{ 2[(1+c^2)(1+\Delta_m^2) + 4c\Delta_m] \}^{1/2}, \end{aligned}$$

where

$$\Delta_m = \int u_{mA}(\mathbf{x}) u_{mB}(\mathbf{x}) d\mathbf{x},$$

c is for the moment arbitrary and may be set to any value between 0 and 1. For the extreme atomic orbital, we use $c=0$ and $Z_m=1.166$; for the intermediate Weinbaum wave function $c=0.256$, $Z_m=1.193$; for the extreme molecular orbital $c=1$, $Z_m=1.193$. The molecular-ion wave function is

$$\phi_b(\mathbf{r}_2; \rho) = N_i^\pm [u_{iA}(2) \pm u_{iB}(2)], \quad (7)$$

where

$$N_i^\pm = 1 / [2(1 \pm \Delta_i)]^{1/2},$$

$$\Delta_i = \int u_{iA}(\mathbf{x}) u_{iB}(\mathbf{x}) d\mathbf{x}.$$

The plus sign refers to leaving the ion in its ground grade state; the minus sign, to leaving the ion in the ungrade state. In Eqs. (6) and (7), u_{mA} and u_{mB} are the ground-state hydrogenic wave functions about nucleus A and B with the effective charge Z_m of the molecule; u_{iA} and u_{iB} are the ground-state hydrogenic wave functions about A and B with the effective charge Z_i of the molecular ion. We make use of the Franck-Condon principle and take the internuclear distance immediately after capture to be the same as before.

In first Born approximation, the prior matrix element of Eq. (2) should equal the post matrix elements provided the unperturbed molecular and ionic wave functions ϕ_m and ϕ_i are exact. However, since we are mainly interested in analyzing the basis of the assumption that $\sigma_A = \frac{1}{2}\sigma_M$, we have made calculations only with the simpler prior interaction and have compared these with the corresponding prior matrix element for the reaction (1a); actually the reaction (1a) is so symmetric that the post and prior matrix elements are identical.

We note further that Eq. (2), which rigorously takes into account electron indistinguishability, has neglected the possibility of proton exchange. Proton exchange would replace $\langle\psi_b|V_i|\psi_a\rangle$ in Eq. (2) by linear combinations of $\langle\psi_b|V_i|\psi_a\rangle$ and other matrix elements, which matrix elements would correspond to the incident proton stripping a hydrogen atom from the H_2 molecule. We have not estimated these stripping matrix elements; probably they are small. Even if they are not insignificant they should be excluded from our calculations because: (i) they have no analog in the BK and JS expressions for σ_A , and (ii) stripping mostly would produce fast H_2^+ ions, which would not be detected in the usual measurements of the cross section for the reaction (1b).

3. THE INTERFERENCE EFFECT

The matrix element in Eq. (2) is integrated over the relative coordinates $\mathbf{r}_1, \mathbf{r}_2, \mathbf{r}_1', \boldsymbol{\rho}$ introduced in Fig. 1. It is trivial to show that the Jacobian of the transformation from this set, together with the center of mass of all five particles, to the laboratory coordinates is unity. In this integration, we keep $\boldsymbol{\rho}$, the internuclear distance fixed, so that the only actual variables are $\mathbf{r}_1, \mathbf{r}_2$, and \mathbf{r}_1' . The matrix element so evaluated corresponds to the capture amplitude for a given orientation of the molecule. Thus

$$\begin{aligned} &\langle\psi_b|V_i|\psi_a\rangle \\ &= \exp(-i\boldsymbol{\alpha}\cdot\boldsymbol{\rho}/2) \int \exp(-i\boldsymbol{\alpha}\cdot\mathbf{r}_1) \exp(i\boldsymbol{\beta}\cdot\mathbf{r}_1') \\ &\quad \times \phi_i^*(\mathbf{r}_2; \boldsymbol{\rho}) u^*(\mathbf{r}_1') V_i \phi_m(\mathbf{r}_1, \mathbf{r}_2, \boldsymbol{\rho}) d\mathbf{r}_1 d\mathbf{r}_2 d\mathbf{r}_1', \quad (8) \end{aligned}$$

where $\boldsymbol{\alpha} = \mathbf{K}_b - \mathbf{K}_a$; $\boldsymbol{\beta} = [M/(M+m)]\mathbf{K}_b - \mathbf{K}_a$. In Eq. (8) $V_i = V_{1C} + V_{AC} + V_{BC} + V_{2C}$; the asterisk signifies the complex conjugate. The matrix element of V_{1C} represents capture of electron 1 by virtue of the interaction between 1 and the incident proton, and is the molecular analog of the BK matrix element for the reaction (1a). Referring to Eq. (6) it is seen that these V_{1C} terms are of two types: those involving $u_{mA}(1) = u_m(\mathbf{r}_1)$ denoted by us as $I_{BK}(A)$, in which the captured electron is associated with proton A; and those involving $u_{mB}(1) = u_m(|\boldsymbol{\rho} + \mathbf{r}_1|)$, denoted by us as $I_{BK}(B)$, in which the captured electron 1 is associated with proton

B. We find

$$\begin{aligned} I_{BK}(A) &= \exp(-i\frac{1}{2}\boldsymbol{\alpha}\cdot\boldsymbol{\rho}) \\ &\quad \times N_i^{\pm} N_m [(c \pm 1)\Delta_{im} + (1 \pm c)\chi_{im}] I_{pe}, \quad (9) \end{aligned}$$

$$\begin{aligned} I_{BK}(B) &= \exp(i\frac{1}{2}\boldsymbol{\alpha}\cdot\boldsymbol{\rho}) \\ &\quad \times N_i^{\pm} N_m [(1 \pm c)\Delta_{im} + (c \pm 1)\chi_{im}] I_{pe}, \\ I_{pe} &= - \int d\mathbf{r}_1 d\mathbf{r}_1' \exp(-i\boldsymbol{\alpha}\cdot\mathbf{r}_1) \exp(i\boldsymbol{\beta}\cdot\mathbf{r}_1') \\ &\quad \times u^*(\mathbf{r}_1') (e^2/r_1') u_m(\mathbf{r}_1), \quad (10) \end{aligned}$$

$$\Delta_{im} = \int u_i^*(x) u_m(x) dx, \quad (11)$$

$$\chi_{im}(\boldsymbol{\rho}) = \int u_i^*(|\mathbf{x} - \boldsymbol{\rho}|) u_m(x) dx.$$

The simplifying assumption that u_i, u_m, u are spherically symmetric has been incorporated into Eqs. (9)–(11).

Evidently

$$I_{BK}(A) = \pm \exp(-i\boldsymbol{\alpha}\cdot\boldsymbol{\rho}) I_{BK}(B). \quad (12)$$

The phase factor $\exp(-i\boldsymbol{\alpha}\cdot\boldsymbol{\rho}) = \exp[i(\mathbf{K}_a - \mathbf{K}_b)\cdot\boldsymbol{\rho}]$ is precisely the phase factor expected from elementary diffraction theory for two identical scattering centers with relative displacement $\boldsymbol{\rho}$. At low energies $\alpha\rho \ll 1$, the amplitudes $I_{BK}(A)$, $I_{BK}(B)$ add constructively for the gerade state and destructively for the ungerade state. This interpretation of the relation (12) suggests that a similar relation should hold for the molecular analog of the atomic JS matrix element, which describes capture of the electron by virtue of the interaction between the incident proton and the proton to which the electron is originally bound. Of course each electron in H_2 is simultaneously bound to both protons, but (as in the V_{1C} matrix element) with the form (6) for ϕ_m it is legitimate to suppose matrix elements involving $u_{mA}(1)$ represent capture of 1 when it is bound to A, while matrix elements involving $u_{mB}(1)$ represent capture of 1 when it is bound to B. Hence in Eq. (8) the molecular analogs of the atomic JS matrix element are: $I_{JS}(A)$, denoting those terms in the matrix element of V_{AC} which involve $u_{mA}(1)$; and $I_{JS}(B)$, denoting those terms in the matrix element of V_{BC} which involve $u_{mB}(1)$. We find

$$\begin{aligned} I_{JS}(A) &= \exp(-i\frac{1}{2}\boldsymbol{\alpha}\cdot\boldsymbol{\rho}) \\ &\quad \times N_i^{\pm} N_m [(c \pm 1)\Delta_{im} + (1 \pm c)\chi_{im}] I_{pp}, \quad (13) \end{aligned}$$

$$\begin{aligned} I_{JS}(B) &= \exp(i\frac{1}{2}\boldsymbol{\alpha}\cdot\boldsymbol{\rho}) \\ &\quad \times N_i^{\pm} N_m [(1 \pm c)\Delta_{im} + (c \pm 1)\chi_{im}] I_{pp}, \\ I_{pp} &= \int d\mathbf{r}_1 d\mathbf{r}_1' \exp(-i\boldsymbol{\alpha}\cdot\mathbf{r}_1) \exp(i\boldsymbol{\beta}\cdot\mathbf{r}_1') \\ &\quad \times u^*(\mathbf{r}_1') (e^2/|\mathbf{r}_1 - \mathbf{r}_1'|) u_m(\mathbf{r}_1), \quad (14) \end{aligned}$$

and observe that Eq. (12) holds for $I_{JS}(A)$, $I_{JS}(B)$, as expected.

The remaining terms in the matrix elements of V_{AC} , denoted by $I_{pp}'(B)$, represent capture of 1 when it is bound to B by virtue of the interaction between C and A ; the remaining terms in the matrix elements of V_{BC} , denoted by $I_{pp}'(A)$, represent capture of 1 when it is bound to A by virtue of the interaction between C and B . We find

$$I_{pp}'(A) = \exp(-i\frac{1}{2}\alpha \cdot \boldsymbol{\rho}) N_{i\pm N_m} [(c\pm 1)\Delta_{im} + (1\pm c)\chi_{im}] I_{pp}'(\boldsymbol{\rho}),$$

$$I_{pp}'(B) = \exp(i\frac{1}{2}\alpha \cdot \boldsymbol{\rho}) N_{i\pm N_m} [(1\pm c)\Delta_{im} + (c\pm 1)\chi_{im}] I_{pp}'(-\boldsymbol{\rho}), \quad (15)$$

$$I_{pp}'(\boldsymbol{\rho}) = \int d\mathbf{r}_1 d\mathbf{r}_1' \exp(-i\boldsymbol{\alpha} \cdot \mathbf{r}_1) \exp(i\boldsymbol{\beta} \cdot \mathbf{r}_1') \times u^*(\mathbf{r}_1') (e^2/|\mathbf{r}_1 - \mathbf{r}_1' + \boldsymbol{\rho}|) u_m(\mathbf{r}_1).$$

$I_{pp}'(A)$ differs from $I_{pp}'(B)$ by the same phase factor as previously, but there is the additional complication that as electron 1 is shifted down (in Fig. 1) from proton A to proton B , the interaction is shifted up. In Eq. (15) this complication shows up in the difference between $I_{pp}'(\boldsymbol{\rho})$ and $I_{pp}'(-\boldsymbol{\rho})$. Similarly we denote by $I_{pe}'(A)$ the terms in the matrix element of V_{2C} which involve $u_{mA}(1)$, by $I_{pe}'(B)$ the terms in the matrix element of V_{2C} which involve $u_{mB}(1)$, and find

$$I_{pe}'(A) = \exp(-i\frac{1}{2}\alpha \cdot \boldsymbol{\rho}) N_{i\pm N_m} \times \int d\mathbf{r}_1 d\mathbf{r}_1' \exp(-i\boldsymbol{\alpha} \cdot \mathbf{r}_1) \exp(i\boldsymbol{\beta} \cdot \mathbf{r}_1') \times u^*(\mathbf{r}_1') V_{pe}'(\mathbf{r}_1, \mathbf{r}_1', \boldsymbol{\rho}) u_m(\mathbf{r}_1),$$

$$I_{pe}'(B) = \pm \exp(i\frac{1}{2}\alpha \cdot \boldsymbol{\rho}) N_{i\pm N_m} \times \int d\mathbf{r}_1 d\mathbf{r}_1' \exp(-i\boldsymbol{\alpha} \cdot \mathbf{r}_1) \exp(i\boldsymbol{\beta} \cdot \mathbf{r}_1') \times u^*(\mathbf{r}_1') V_{pe}'(\mathbf{r}_1, \mathbf{r}_1', -\boldsymbol{\rho}) u_m(\mathbf{r}_1), \quad (16)$$

$$V_{pe}'(\mathbf{r}_1, \mathbf{r}_1', \boldsymbol{\rho}) = - \int d\mathbf{r}_2 [u_i(\mathbf{r}_2) \pm u_i(\mathbf{r}_2 + \boldsymbol{\rho})] (e^2/|\mathbf{r}_1 - \mathbf{r}_1' - \mathbf{r}_2|) \times [u_m(\mathbf{r}_2 + \boldsymbol{\rho}) + c u_m(\mathbf{r}_2)].$$

The terms $I_{pp}'(A)$, $I_{pp}'(B)$, $I_{pe}'(A)$, $I_{pe}'(B)$ together represent capture of electron 1 from one of the atoms by virtue of the interaction between the incoming proton and the other atom. Such capture has no analogue in the atomic reaction (1a), and is not estimated by us. The contributions from I_{pe}' and I_{pp}' should be smaller than the contributions from I_{pe} and I_{pp} , and perhaps should be omitted entirely in view of recent results⁹ concerning the atomic proton-proton contribution. At intermediate energies these first Born approximation matrix elements (15)–(16) are by no means negligible compared to (13)–(14) however.

4. THE MOLECULAR BK CONTRIBUTION

The molecular BK contribution is found from Eq. (2), replacing the entire matrix element $\langle \psi_b | V_i | \psi_a \rangle$ by its BK parts $I_{BK}(A) + I_{BK}(B)$, Eq. (9). Thus

$$\frac{d\sigma_{MBK}}{d\Omega} = 2 \left[\left(\frac{\mu_a \mu_b}{2\pi \hbar^2} \right)^2 \frac{K_b}{K_a} \right] 2(N_{i\pm N_m})^2 \times \{ [\Delta_{im} \pm \chi_{im}(\boldsymbol{\rho})] (1 \pm c) \}^2 \times [1 \pm j_0(\alpha\rho)] |I_{pe}|^2, \quad (17)$$

where j_0 is the spherical Bessel function of zeroth order. The j_0 term arises from the interference between $I_{BK}(A)$ and $I_{BK}(B)$. Equation (10) yields

$$I_{pe} = \left(E_a - \frac{\hbar^2 \beta^2}{2\mu} \right) g_m(\boldsymbol{\alpha}) g^*(\boldsymbol{\beta}), \quad (18)$$

with

$$g_m(\boldsymbol{\alpha}) = \int d\mathbf{r} u_m(\mathbf{r}) \exp(-i\boldsymbol{\alpha} \cdot \mathbf{r}), \quad (19)$$

$$g(\boldsymbol{\beta}) = \int d\mathbf{r} u(\mathbf{r}) \exp(-i\boldsymbol{\beta} \cdot \mathbf{r}),$$

and $E_a = -e^2/2a_0$, $\mu = mM(m+M)^{-1}$; a_0 is the Bohr radius.

The angular dependence of the differential cross section is contained in the magnitudes of $\boldsymbol{\alpha}$ and $\boldsymbol{\beta}$. In terms of the scattering angle θ

$$\alpha^2 = K_b^2 + K_a^2 - 2K_b K_a \cos\theta = K_a^2 [1 + (K_b/K_a)^2 - 2(K_b/K_a) \cos\theta]. \quad (20)$$

The energy conservation is given by

$$(\hbar^2 K_a^2 / 2\mu_a) = (\hbar^2 K_b^2 / 2\mu_b) + \Delta E,$$

where $E(\text{atom}) + E(\text{ion}) - E(\text{molecule}) = \Delta E \cong 2$ eV is the difference in internal energies between the initial and the final states, and may be neglected in comparison with the kinetic energy of the total system. Hence

$$(K_b/K_a) = (\mu_b/\mu_a)^{\frac{1}{2}}. \quad (21)$$

Using $\mu_a = M$, $\mu_b = M+m$, and neglecting terms of higher order in m/M

$$\alpha^2 = K_a^2 \left(\frac{m}{M} \right)^2 \left[\frac{1}{4} + \left(\frac{2 \sin\theta/2}{(m/M)} \right)^2 \right] = \left(\frac{mv}{2\hbar} \right)^2 (1 + 4\lambda), \quad (22)$$

where

$$\lambda = [2(M/m) \sin^2 \frac{1}{2} \theta]^2. \quad (23)$$

The reason for the introduction of the new angle variable λ is to facilitate calculation, since λ has the convenient limits of zero and $4(M/m)^2$, and the upper limit $4(M/m)^2$ may straight away be replaced by infinity. It also is easy to verify that $\beta^2 = \alpha^2$ to the order of approximation of Eqs. (21)–(23).

With this new notation, the elementary solid angle is given by

$$d\Omega = \frac{1}{2} (m/M)^2 d\lambda d\phi, \quad (24)$$

and one finds, after evaluating g_m and g , Eq. (19), that to lowest order in m/M

$$\frac{1}{2}\sigma_{\text{MBK}} = 2^7 \pi a_o^2 (N_i \pm N_m)^2 [\Delta_{im} \pm \chi_{im}(\rho)]^2 (1 \pm c)^2 \times Z_m^5 [F(n) \pm G(n, \rho)] (1/n^{12}), \quad (25)$$

where

$$n = \hbar v / 2e^2,$$

$$F(n) = 4 \int_0^\infty \frac{d\lambda}{[n^{-2} + (1+4\lambda)]^2 [Z_m^2 n^{-2} + (1+4\lambda)]^4}, \quad (26)$$

$$G(n, \rho) = 4 \int_0^\infty \frac{j_0[(\rho/a_o)n(1+4\lambda)^{1/2}] d\lambda}{[n^{-2} + (1+4\lambda)]^2 [Z_m^2 n^{-2} + (1+4\lambda)]^4}.$$

The integral $F(n)$ easily can be evaluated and expressed in closed form. The other integral $G(n, \rho)$ has been integrated numerically. Figure 2 shows a plot of $F(n)$ and $G(n, \rho)$ as a function of n , using a value of $\rho = 0.74$ A.

Equation (25) shows that σ_{MBK} consists of two parts. The first term $F(n)$ increases with n and eventually reaches an asymptotic value for large enough n . The cross section will then simply decrease with incident velocity as the factor v^{-12} . The term $G(n, \rho)$, which vanishes as either ρ or n approach infinity, expresses the interference of the two capture amplitudes associated with the two proton centers in the molecule. As always, the plus and minus signs refer to transitions to the gerade and the ungerade states, respectively. In the limit of very large internuclear distances, transitions to the gerade and the ungerade states must be equally probable. Indeed, as $\rho \rightarrow \infty$: Z_m and $Z_i \rightarrow 1$; $\Delta_{im} \rightarrow 1$; Δ_m, Δ_i , and $\chi_{im} \rightarrow 0$; $c \rightarrow 0$; and for either sign Eq. (26) reduces to

$$\frac{1}{2}\sigma_{\text{MBK}} = 2^5 \pi a_o^2 \frac{n^{-12}}{(1+n^{-2})^5}, \quad (27)$$

which is precisely half σ_{ABK} . At the true internuclear distance $\rho = 0.74$ A however, the values of Δ_{im} , χ_{im} , and c are such that $(\Delta_{im} - \chi_{im})(1 - c)$ is considerably less than $(\Delta_{im} + \chi_{im})(1 + c)$. Thus, referring to Eq. (25), even in the absence of interference, transitions to ungerade states are much less probable than transitions to gerade states; at energies less than 400 kev, where F and G have the same sign (Fig. 2), interference further reduces the relative probability of transition to ungerade states.

Since the internuclear spacing is of the order of 10^4 times the de Broglie wavelength of the proton at an incident energy of 400 kev, persistence of significant interference to such high energies is somewhat surprising. To understand this, let us consider the special case that the nuclear protons lie perpendicular to the direction of the incident proton. Then the criterion for

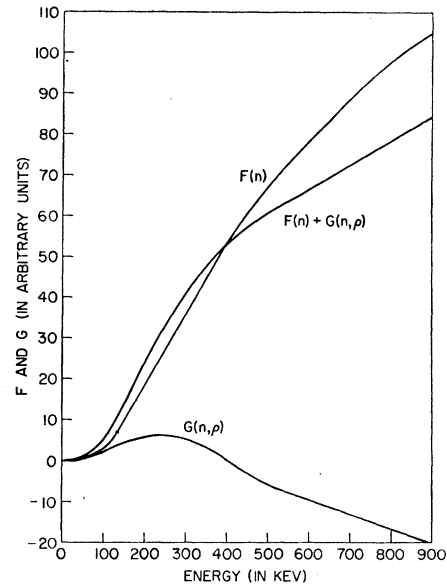


FIG. 2. The functions $F(n)$ and $G(n, \rho)$ which, respectively, represent the direct and the interference terms in the capture cross section are given in arbitrary units as functions of incident proton energy. Note how the interference term $G(n, \rho)$ turns negative at about 400 kev. The experimental value of 0.74 A is used for ρ .

interference would be $K\rho \sin\theta < \sim 1$, where $K = Mv/\hbar$. Because m/M is so small the incident proton is almost undeflected however; in fact the mean value of $\sin\theta$ is $\sim m/M$. Consequently the criterion for interference becomes $mvp/\hbar < \sim 1$, i.e., the effective wavelength determining the interference is not the wavelength of a proton at the incident proton velocity, but the 2000 times larger wavelength of an electron at that velocity. To put it more formally, Eqs. (8) and (22) show that the effective wave number is not K_a , but rather $|K_b - K_a| \cong mvp/\hbar$.

Figure 3 shows two sets of curves. The upper set of curves (I) compares our theoretical $\frac{1}{2}\sigma_{\text{MBK}}$ (solid line) with σ_{ABK} (dashed line); the small contribution to the total cross section from transitions to ungerade states has been neglected, i.e., Fig. 3 is computed using only the plus sign in Eq. (25). The close agreement between $\frac{1}{2}\sigma_{\text{MBK}}$ and σ_{ABK} at energies $< \sim 400$ kev ($v < \sim 9 \times 10^8$ cm/sec) appears to be a fortuitous result of the combination of factors occurring in Eq. (25). For example $Z_m \cong 1.17$ rather than unity, as in atomic H, and $(1.17)^5 = 2.2$; consequently the Z_m^5 dependence of $\frac{1}{2}\sigma_{\text{MBK}}$ on Z_m at high energies [$Z_m^2 n^{-2} \ll 1$ in Eq. (26)] makes $\frac{1}{2}\sigma_{\text{MBK}}$ about twice as large as it would be if Z_m were equal to one. We see no logical reason why the assumption that $\frac{1}{2}\sigma_{\text{MBK}} = \sigma_{\text{ABK}}$, if it were based on sound physical reasoning, should require that $Z_m \cong 1.17$. The divergence between $\frac{1}{2}\sigma_{\text{MBK}}$ and σ_{ABK} at energies exceeding 400 kev results from the onset of destructive interference in transitions to the gerade state.

In the energy range below 1 Mev, the differences between results obtained with the three different types of

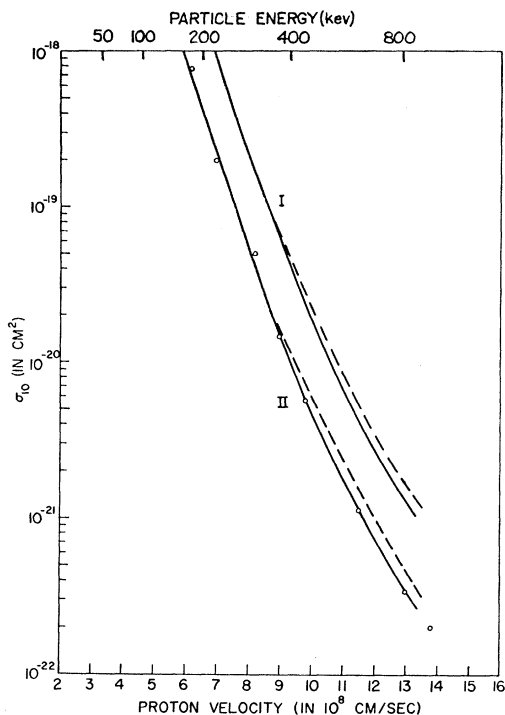


FIG. 3. Capture cross section as a function of incident proton velocity. The circles are the experimental data of Barnett and Reynolds. The upper set of curves (I) indicate the theoretical cross sections without p - p interactions, while the lower set (II) takes this into consideration in the manner as given in the text.

wave functions—extreme atomic orbital (Wang¹⁶), Weinbaum, and extreme molecular orbital—are almost indiscernible on the scale of Fig. 3. In the limit $v \rightarrow \infty$ these differences are more appreciable, though still not large, as can be inferred from the first row of Table I, which for each of the different wave functions lists the high-energy limit of the ratio $\frac{1}{2}\sigma_{MBK}/\sigma_{ABK}$. Of the three wave functions, the extreme molecular orbital has the highest electron density at the center of the molecule (as can be seen by plotting the electron distributions) and also has the largest capture cross section in the high-energy limit, followed by the Weinbaum with the next highest density. From the uncertainty principle, the most highly localized wave function should have the largest high momentum components. The remarks of this paragraph and the three preceding, taken together with Eqs. (17)–(19) and (22), justify many of the assertions concerning effects (i)–(iii) which were made in Sec. 1.

5. THE MOLECULAR JS CONTRIBUTION

The molecular cross section analogous to σ_{AJS} is obtained when $\langle \psi_b | V_i | \psi_a \rangle$ in Eq. (2) is replaced by $I_{BK}(A) + I_{BK}(B) + I_{JS}(A) + I_{JS}(B)$, Eqs. (9) and (13). Since I_{BK} and I_{JS} obey the identical relation (12), it is evident that $d\sigma_{MJS}/d\Omega$ is given by Eq. (17), provided $|I_{pe}|^2$ is replaced by $|I_{pe} + I_{pp}|^2$. In other words the

interference and other qualitative features of the molecular cross section discussed in the previous section hold for σ_{MJS} as well as for σ_{MBK} . In fact Eq. (25) holds for $\frac{1}{2}\sigma_{MJS}$ provided the integrands of $F(n)$ and $G(n, \rho)$, Eq. (26), are made consistent with the replacement of $|I_{pe}|^2$ by $|I_{pe} + I_{pp}|^2$. As in the previous section, it readily is shown that $\frac{1}{2}\sigma_{MJS} = \frac{1}{2}\sigma_{AJS}$ for transitions to either gerade or ungerade states in the limit $\rho \rightarrow \infty$. I_{pp} , Eq. (14), can be evaluated in closed form from expressions given by Lewis²⁰; however $\frac{1}{2}\sigma_{MJS}$ was not computed exactly at all energies, for reasons explained previously. The lower set of curves (II) in Fig. 3 compares σ_{AJS} (dashed line) with our theoretical $\frac{1}{2}\sigma_{MJS}$ (solid line) computed as described in Sec. 1. The circles are the experimental points of Barnett and Reynolds.¹⁴ The agreement between the magnitudes of our estimated $\frac{1}{2}\sigma_{MJS}$ and the measured $\frac{1}{2}\sigma_M$ is much closer than it has any right to be, as discussed in Sec. 1. The second row of Table I lists the high-energy limit of the ratio $\frac{1}{2}\sigma_{MJS}/\sigma_{AJS}$. The third row shows that the high-energy limit of $\frac{1}{2}\sigma_{MJS}/\frac{1}{2}\sigma_{MBK}$ is almost identical with the high-energy limit of $\sigma_{AJS}/\sigma_{ABK} = 0.661$, which is merely another way of saying that $\frac{1}{2}\sigma_{MJS}/\sigma_{AJS}$ is almost identical with $\frac{1}{2}\sigma_{MBK}/\sigma_{ABK}$.

6. TRANSITIONS TO UNGERADE STATES

So far we have assumed that transitions to ungerade states are unimportant. The experiments of Keene¹¹ seem to support this assumption, at least at energies of the order of 15 keV. In this section, we will consider the transition to ungerade states at all energies. From Eq. (25) we obtain the following relative ratio for dissociation

$$\frac{\frac{1}{2}\sigma_{MBK}^-}{\frac{1}{2}\sigma_{MBK}^+} = \frac{[(\Delta_{im} - \chi_{im})(1-c)]^2(1+\Delta_i)(F-G)}{[(\Delta_{im} + \chi_{im})(1+c)]^2(1-\Delta_i)(F+G)}, \quad (28)$$

where of course $\frac{1}{2}\sigma_{MBK}^+$ is the cross section to gerade states plotted in Fig. 3 and tabulated in Table I. This ratio is energy dependent, and varies very drastically with different types of molecular wave functions. For the extreme molecular orbital $c=1$, this ratio is zero at all energies. For the other two types of wave functions, the ratio is very small at low energies ($< \sim 100$ keV) since $G(n, \rho)$, at low energies, is close to $F(n)$ (see Fig. 2). The ratio becomes more appreciable when $G(n, \rho)$ becomes negative. This is especially true with the Wang extreme atomic orbital wave function for which the

TABLE I. Cross-section ratios in the high-energy limit.

Ratios	Extreme atomic	Weinbaum	Extreme molecular
$\frac{1}{2}\sigma_{MBK}/\sigma_{ABK}$	1.223	1.421	1.439
$\frac{1}{2}\sigma_{MJS}/\sigma_{AJS}$	1.255	1.468	1.486
$\frac{1}{2}\sigma_{MJS}/\frac{1}{2}\sigma_{MBK}$	0.678	0.683	0.683

²⁰ R. R. Lewis, Phys. Rev. **102**, 537 (1956).

ratio reaches a peak value of about 28% at 900 kev. In the high-energy limit, however, $G(n,\rho)$ vanishes and the ratio is just a ratio of two constants and will no longer be energy dependent. We then have

$$\frac{\frac{1}{2}\sigma_{\text{MBK}}^-}{\frac{1}{2}\sigma_{\text{MBK}}^+} \xrightarrow{v \rightarrow \infty} \frac{[(\Delta_{im} - \chi_{im})(1-c)]^2(1+\Delta_i)}{[(\Delta_{im} + \chi_{im})(1+c)]^2(1-\Delta_i)} \quad (29)$$

For the Wang wave function, the ratio at the high-energy limit is about 19%; for the Weinbaum, about 7%. Figure 4 shows a plot of this ratio against energy. Curve *I* is plotted for the Wang wave function; curve *II* for the Weinbaum; the straight lines *A* and *B* indicate, for the Wang and Weinbaum, respectively, the high-energy limit ratios computed from Eq. (29). The maximum at 900 kev is due entirely to the fact that at this energy the destructive interference in the gerade transitions (and the corresponding constructive interference in the ungerade transitions) is most pronounced. A further increase of incident energy decreases the ratio, which thereafter oscillates slowly and with rapidly decreasing amplitude about the high-energy limit ratio.

The fact that the projection onto ungerade states of the molecular-ion is zero when we employ the extreme molecular orbital wave function can be easily understood, since the extreme molecular orbital is nothing more than a product of two gerade (extreme) molecular-ion wave functions.

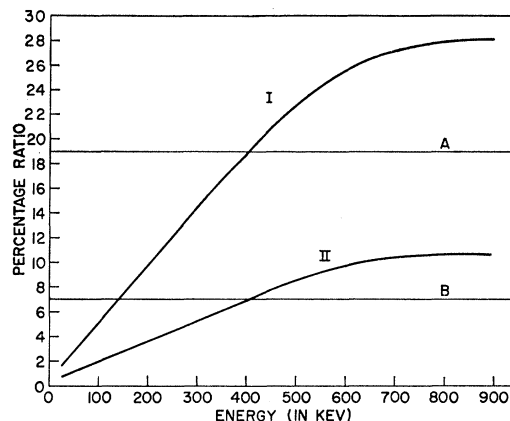


FIG. 4. The ratio of capture cross section corresponding to transition to ungerade states to the transition to gerade states. Curve *I* shows the ratio for the Wang extreme atomic orbital wave function, and curve *II* for the Weinbaum. The straight lines *A* and *B* indicate the high-energy limit cross-section ratios for the Wang and the Weinbaum wave functions, respectively.

The results which have been quoted in this section remain essentially unaltered when $\sigma_{\text{MJS}}^{\pm}$ are substituted for $\sigma_{\text{MBK}}^{\pm}$.

ACKNOWLEDGMENTS

We are indebted to Dr. Richard M. Drisko, Dr. T. M. Donahue, and Dr. Robert H. Bassel for many helpful discussions.

Photodisintegration of the Deuteron with 94-Mev Bremsstrahlung Radiation*†

J. A. GALEY‡

The Enrico Fermi Institute for Nuclear Studies, The University of Chicago, Chicago, Illinois

(Received August 24, 1959)

Differential cross sections for the reaction $\gamma + d \rightarrow p + n$ have been determined at laboratory angles of 45°, 75°, 90°, and 135° for laboratory photon energies from approximately 50 to 90 Mev. At each of the above angles the energy spectrum of the recoil protons was determined with a counter telescope and a pulse-height analysis system. The low cross section for this reaction necessitates the reduction of background to a minimum. This was accomplished by the use of a gaseous target and a particle selection technique. The differential cross sections and the estimates of the parameters describing angular distributions are in reasonable agreement with recent calculations by de Swart and Marshak and by Zernik, Rustgi, and Breit.

I. INTRODUCTION

ALONG with single and multiple nucleon-nucleon scattering and the n - p capture process, the photodisintegration of the deuteron constitutes a possible

source of information on two-body nuclear interactions. It is unique in the photonuclear field, because the matrix elements describing the process are more readily calculated than those involved in gamma-ray interactions with more complex nuclei. In addition, being a two-body interaction the determination of the energy and the angle of recoil of the proton (or the neutron) uniquely fixes the energy of the photon initiating the reaction.

The energy range from 20 Mev on up where effective range theory is not satisfactory has been investigated

* Research supported by a joint program of the Office of Naval Research and the U. S. Atomic Energy Commission.

† A thesis submitted to the Department of Physics, the University of Chicago, in partial fulfillment of the requirements for the Ph.D. degree. A more complete account of the method of data reduction and of sources of error is given in the thesis filed with the Department of Physics, University of Chicago.

‡ Present address: Department of Physics, University of Notre Dame, Notre Dame, Indiana.